




XFF TN: 805660  
Western Libraries Interlibrary Loan - XFF

XFF ILLiad TN: 805660   
Lending String: \*XFF,AD#,TFW,YTM  
Delivery Options:

- Scan to Odyssey - Rapid

Location: **Wilson 1E - Periodicals**  
Call No.: **TK5981 .A83**


Journal Title: Journal of the Audio Engineering Society.  
Vol: 38 Iss: 9  
Month/Year: 9 1990  
Pages: 653-666  
Article Author: Audio Engineering Society. HENRIQUEZ, JA,  
Article Title: A PHASE-LINEAR AUDIO EQUALIZER - DESIGN AND IMPLEMENTATION  
Imprint: [New York, etc.] Audio Engineering Society.

**Western Washington University**  
Wilson Library - XFF  
Bellingham, WA 98225-9103  
Phone 360-650-3076 FAX 360-650-3954  
E-Mail illiad@wwu.edu

  
IL / Rapid Number: 221411459

Borrowing Library Information:  
libill@uno.edu

OCLC Symbol: LNU  
Patron:

Borrower's TN: 5949617  


Max Cost: 0.00IFM

Shipping Information:

ILL - Earl K Long Library - MSY 24  
University of New Orleans  
2000 Lakeshore Drive  
New Orleans, Louisiana 70148  
United States

Odyssey: louis-odyssey.hosts.atlas-sys.com  
Fax: 504-280-3173  
Email: libill@uno.edu

**NOTICE: Warning Concerning Copyright Restrictions:**

The copyright law of the United States (Title 17, United States Code) governs the making of photocopies or other reproductions of copyrighted material.

Any electronic copy or copies, photocopies or any other type of reproduction of this document or distribution of this copyrighted material may be an infringement of the Copyright Law.

This copy is not to be used for any purpose other than private study, scholarship, or research (section 107). "If a user makes or later uses any form of reproduction from this copyrighted work for purposes in excess of section 107, Fair Use, that user may be liable for copyright infringement."

If there are any quality control issues with this document please contact us as soon as possible.

ILLiad@wwu.edu

**Date Received:**

**Pages are:** Missing      Cut Off      Other  
(Please circle the appropriate description)      top bott left right

**Page Numbers:**

strument Division of the U.S. Weather Bureau, where she worked until her impending marriage to Charles H. Corliss, to which the Bureau objected. She realized her childhood ambition of becoming an astronomer at the U.S. Naval Observatory, but found her work to be largely computation. In 1944 she joined the Sound Section at the National Bureau of Standards. During 1962 and 1963, she worked as a guest in the Electrical Engineering Department at Imperial College in London, England, under Professor E. Colin Cherry.

Mrs. Corliss has published primarily in the fields of hearing measurement and speech communication. Research into the problem of measuring speech signals led her to author several publications on the general subject of measuring transient phenomena. In her study of the resolution limits for measurements on oscillatory systems, she found that the theoretical developments permitted assessment of the behavior of the ear as a speech communication channel. For a number of years she conducted a hearing aid testing program, a service supplied by the National Bureau of Standards to the Veterans Administration. This led to the development of a quantitative assessment for the problems of hearing impairment, of which the present paper is a consequence.

As a result of her activities on environmental matters (she is presently chairman of the Subcommittee on Environmental Quality of the IEEE's Energy Committee) she and her colleague at the National Bureau

of Standards, Raymond D. Berendt, together with Maurice Ojalvo from the National Science Foundation published NBS Handbook 119 "Quieting: A Practical Guide to Noise Control."

Some of her more recent work has been concerned with improving the accuracy of tests for diagnosing hearing impairment and assessing the assistance provided by hearing aids.

In 1980, she retired from the National Bureau of Standards and helped to set up Forest Hills Laboratory, on whose behalf she has continued some work on hearing; but she has also branched out into studies of musical instruments and instrumentation for assessing their transient and resonance characteristics.

Mrs. Corliss is a Fellow of the Acoustical Society of America, and of the Washington Academy of Sciences. In addition, she is a member of the American Physical Society, the Institute of Electrical and Electronic Engineers, and the Catgut Acoustical Society. In 1972-75 she served on the Executive Council of the Acoustical Society of America, and was Vice-President of the Acoustical Society from 1978-80. At present she is serving as Vice-President for Affiliated Societies in the Washington Academy of Sciences. As part of her concern about hearing impairment, she is an affiliated member of the Washington Area Group for the Hard of Hearing.

Along the way, the Corlisses have raised two sons, one of them now a mechanical engineer working on jet engines, and the other studying to be a chef.

# A Phase-Linear Audio Equalizer: Design and Implementation\*

JUAN A. HENRIQUEZ, TERRY E. RIEMER, AND RUSSELL E. TRAHAN, JR.

*Department of Electrical Engineering, University of New Orleans, New Orleans, LA 70148, USA*

The design and implementation of an 11-band phase-linear digital audio equalizer system based on digital signal processing techniques is presented. The design of analog Bessel–Thomson and digital FIR filters for the preservation of phase linearity, and the use of oversampling and decimating techniques resulting in a robust system feasible for hardware implementation are included. Techniques resulting in filter size reduction and in flat composite frequency response (whenever two or more adjacent bands are added together) are also described. The problems encountered in this design can be found in the development of any digital audio system, and the techniques used to solve them could also be efficiently implemented in the development of a system other than the digital equalizer.

## 0 INTRODUCTION

The motivation for designing a digital audio equalizer arises from the desire to resolve the shortcomings usually associated with analog counterparts, such as phase nonlinearities, and a lack of independent gain control (boost or cut) for the series of bandpass/reject filters tuned at some specified frequency. Phase nonlinearities are present in analog equalizers where they usually appear in the portion of the frequency spectrum where boost or cut is applied. Sensitivity of the human ear to phase nonlinearities has been demonstrated experimentally (see, for example, [1]). When uncorrelated errors are introduced independently into one or more sources in a multipoint acoustic field (such as in a multi-track recording session), the audio image can be severely degraded because phase information provides a sense of the relative position of the audio source. On the other hand, lack of independent gain control results in interband gain dependence and becomes more evident when all bands are at maximum boost or cut. Even in the best of equipment, gain variations in one band can influence adjacent bands and lead to amplitude devia-

tions far away from a desired flat response. At the same time, phase nonlinearities in one band can be affected by the gain setting of adjacent bands. See, for example, the frequency response shown in Fig. 1.

This paper describes a design that makes possible the implementation of a digital audio equalizer which allows for the independent gain adjustment of a particular band without affecting adjacent bands and which is phase linear for any combination of frequency-band gains. A digital equalizer will furthermore have the advantage of providing a very wide dynamic range, long-term accuracy, and stability by the use of sophisticated microprocessor control and decimating/oversampling techniques.

### 0.1 Phase Linearity

It is commonly accepted that when phase nonlinearities are introduced into monaural sound sources, the effects are inaudible. However, when such errors are introduced independently into one or more sources in a multipoint acoustic field, the audio image can be severely distorted. Since the ability of the human brain to determine the direction and location of the audio source depends on the information conveyed not only by the magnitude but also by the phase of the perceived signal, any uncorrelated changes to the phases of each

\* Manuscript received 1989 December 16; revised 1990 March 19.

source in a multipoint acoustic field will result in a distorted audio image. The phase-linearity property guarantees that no matter what linear combination of channels is combined, the result will be phase linear. Therefore it is commonly acceptable among audiophiles (at least in theory) that the criteria for high-fidelity performance of an audio system should not only comprise a transfer function which preserves the shape of the input waveform, but also linearity of phase.

In the time domain, a measure of distortion introduced by phase nonlinearities is given by the group delay, denoted here by  $\sigma$  and defined as the negative of the slope of the phase response, or

$$\sigma = - \frac{d}{d\omega} \theta(\omega) \quad (1)$$

where

$\sigma$   $\triangleq$  group delay

$\theta(\omega)$   $\triangleq$  waveform phase response

$\omega$   $\triangleq$  radian frequency

$\frac{d}{d\omega}$   $\triangleq$  derivative with respect to frequency.

Consider for instance an audio signal passing through a given filter system. If all the frequencies in the audio spectrum (harmonics plus fundamentals) take the same amount of time to pass through such a filter, then the given system has a constant group delay and is considered phase linear. If, on the other hand, a frequency-dependent delay exists and some frequencies take longer to pass than others (the effect of a nonconstant group delay), then the given system is considered not phase linear.

In [2] the effects of phase nonlinearities introduced by digital filters in commercial digital recorders have been studied. The analysis of group delay shows that typical recording systems exhibit a nonlinear rise above 5 kHz, reaching a delay of 300  $\mu$ s at 20 kHz. For high frequencies, the delay is not a constant, and as a result, the output signal will be dispersed in time since the notes will no longer begin simultaneously. This explains in part the lack of bass response and the high-frequency content usually associated with some CD recordings.

Fortunately, in the time domain the problems associated with phase nonlinearities can be virtually eliminated by the implementation of nonrecursive finite impulse response (FIR) digital filters and analog Bessel-Thomson filters.

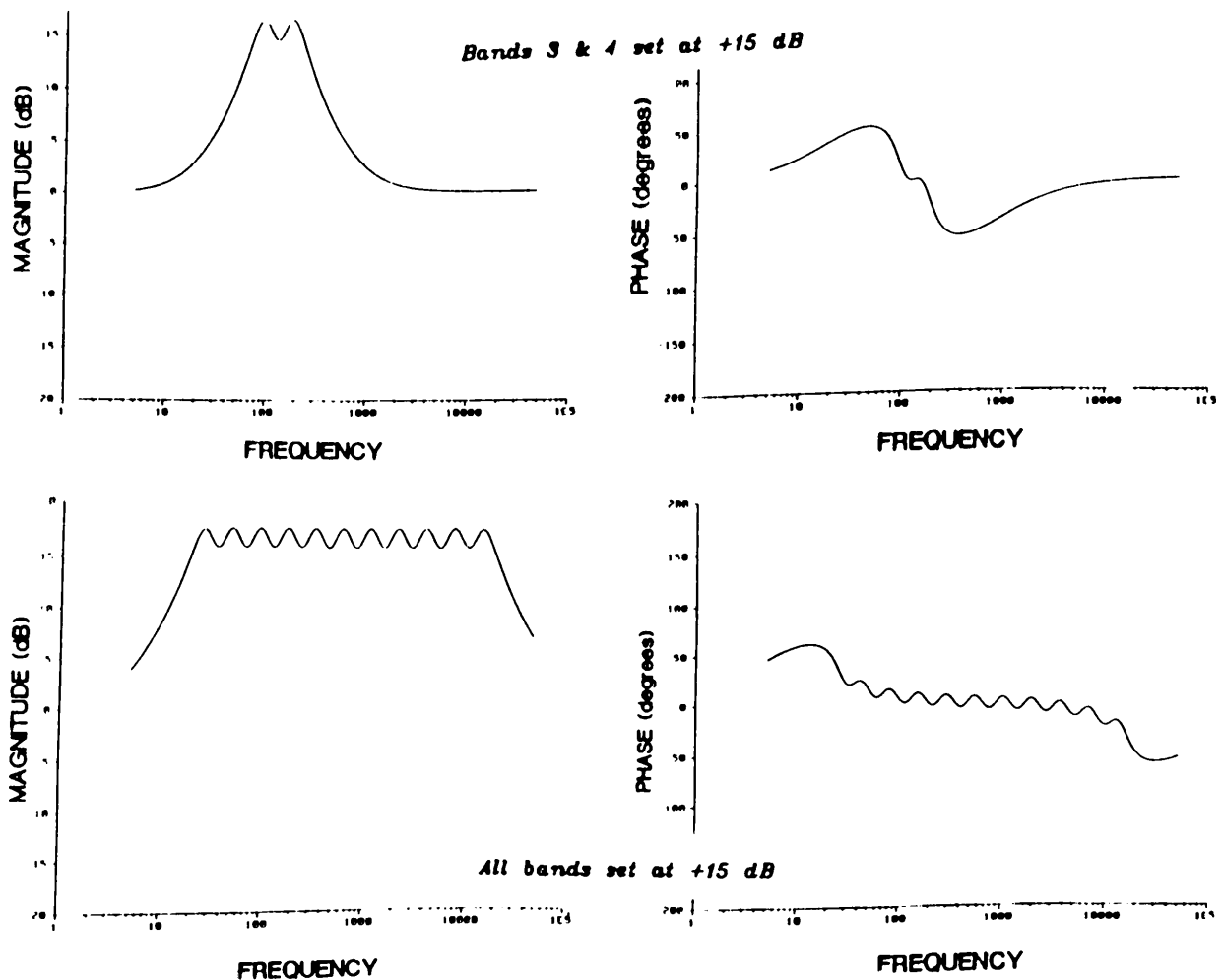


Fig. 1. Magnitude and phase response (simulated through SPICE) for top-of-the-line 11-band analog equalizer, showing deviations from flat response and phase nonlinearities associated with typical analog design.

## 0.2 System Overview

The method presented here consists of a parallel filter structure which divides the audio spectrum into four separate bands, each sampled at an integer multiple of 44.1 kHz. The study separates the system design into three major sectors:

1) *Input stage*. Includes analog-to-digital (A/D) conversion, oversampling, and design of anti-aliasing and decimator filters [see Fig. 2(a)].

2) *Equalizer stage*. Includes the design of symmetric digital FIR filters for all 11 bands of the equalizer [see Fig. 2(b)].

3) *Output stage*. Includes oversampling, digital-to-analog (D/A) conversion, and design of anti-imaging and interpolator filters [see Fig. 2(c)].

At the input, oversampling (up to three times the base frequency of 44.1 kHz) is used to reduce the order of a set of phase-linear Bessel–Thomson anti-aliasing filters (one for each audio path). After A/D conversion, this process is followed by a set of digital anti-aliasing FIR filters and by the reduction of the sampling rate (or decimation). This last step is needed in order to match the sampling frequency corresponding to each parallel filter path of the equalizer stage (Fig. 3). Each band is implemented by a set of linear-phase FIR filters adjustable to  $\pm 16$  dB of gain, and each filter is sampled at an integer multiple of the nominal frequency of 44.1 kHz. The main criterion in choosing these sampling rates has been to keep the number of filter coefficients as low as possible while considering other parameter constraints such as cutoff frequencies and stopband/passband attenuation.

At the output, a function similar to the anti-aliasing filter must be performed by a low-pass filter known as anti-imaging filter. Samples coming from the equalizer stage at 44.1 kHz must be converted to analog form and then low-pass filtered in order to remove the ultrasonic frequencies [see Fig. 2(c)]. The function of the anti-imaging filter is to eliminate the spectral images produced by the D/A conversion process at multiples of the sampling frequency. The energy of such images is not audible, but their presence may cause modulation in other equipment connected to the system, or it may lead to unwanted distortion. Our design criterion is then to obtain an anti-imaging filter which is flat in the passband, with sharp cutoff and high rolloff rate, and which is phase linear. As shown later, the order of this filter is very high. However, the number of poles can be reduced by implementing a digital oversampling filter previous to the D/A process. For our system, a digital filter can be implemented to perform 3 times oversampling (at 132.30 kHz), thus reducing the order of the Bessel–Thomson filter used considerably.

In Sec. 1 we examine the basic theory of FIR filters and introduce expressions for the computation of their frequency response. Sec. 2 establishes the system filter requirements and the parameters involved in the design of FIR filters. In Sec. 3 the design of FIR filters is studied, and the problems encountered in the devel-

opment of the digital equalizer system are presented. This section also explains the techniques used in solving these difficulties. Sec. 4 brings all the system requirements together and explains how they are obtained. It also includes several examples illustrating the performance of the equalizer system. Secs. 5 and 6 include the proposed hardware and the conclusions, respectively.

## 1 FINITE IMPULSE RESPONSE FILTERS

An FIR filter of duration  $N$  is defined as one having the following impulse response:

$$h(n) = \begin{cases} \alpha_n, & 0 \leq n \leq N - 1 \\ 0 & \text{elsewhere} \end{cases} \quad (2)$$

where  $\alpha$  represents the impulse response coefficient and  $n$  is an integer. For the type of design we are considering, the impulse response must satisfy the following symmetry condition which guarantees linearity of phase:

$$h(n) = h(N - 1 - n), \quad n = 0, 1, \dots, N - 1 \quad (3)$$

where  $N - 1$  represents the order of the function and  $N$  can be even or odd. Eq. (3) implies that the impulse response of an FIR filter is limited to a finite number of points [as opposed to an infinite impulse response (IIR) filter, which requires an infinite number of coefficients and which is also not phase linear]. Note that if no coefficients  $\alpha$  are missing in Eq. (2), a function of order  $N - 1$  will have  $N$  terms in its impulse response.

In the  $z$  domain an FIR filter can be characterized by a transfer function  $H(z)$ , where

$$H(z) = \sum_{n=0}^{N-1} h(n)z^{-n} \quad (4)$$

This equation describes a polynomial in  $z^{-1}$  of degree  $N - 1$ . Thus  $H(z)$  has  $N - 1$  zeros that can be located anywhere in the finite  $z$  plane and  $N - 1$  poles, all lying at  $z = 0$  [3].

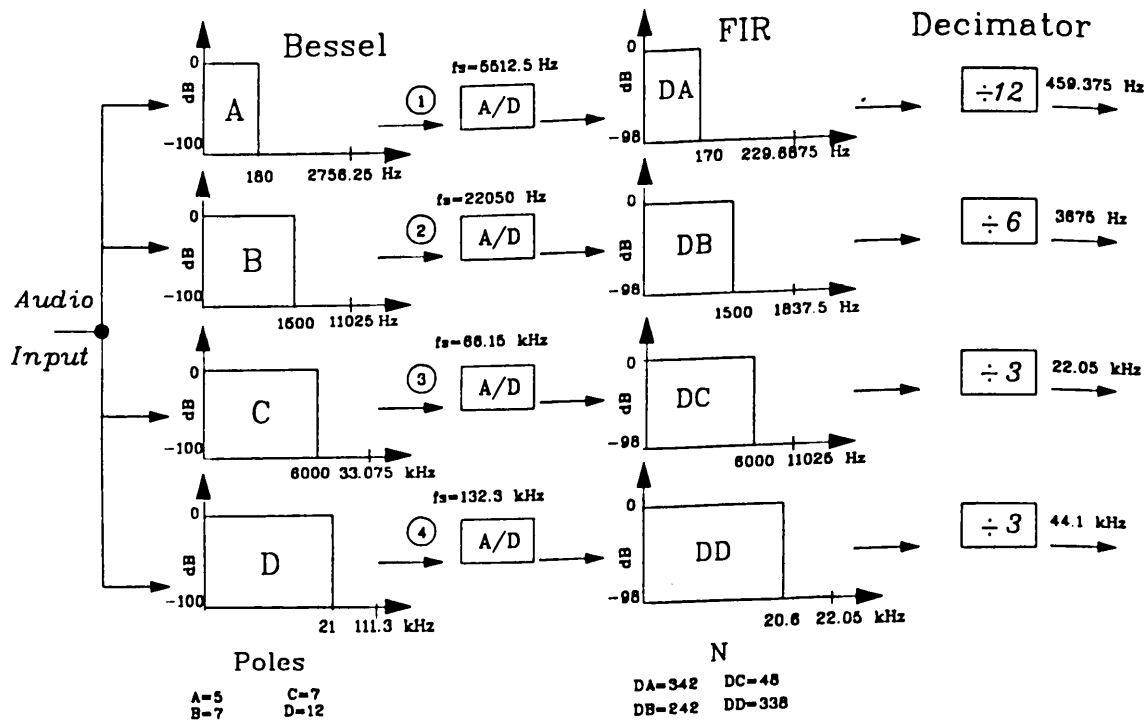
In terms of its frequency response Eq. (4) becomes

$$H(e^{j\omega}) = \sum_{n=0}^{N-1} h(n)e^{-j\omega n} \quad (5)$$

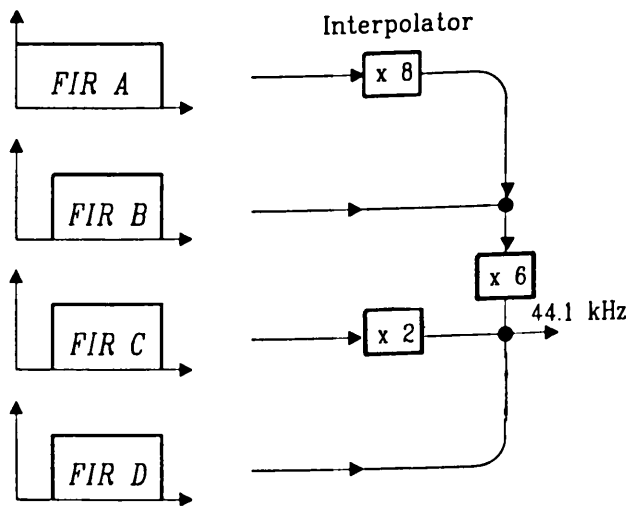
The frequency response of a linear-phase FIR filter can be expressed as

$$H(e^{j\omega}) = \hat{H}(e^{j\omega}) e^{j(\beta - \sigma\omega)} \quad (6)$$

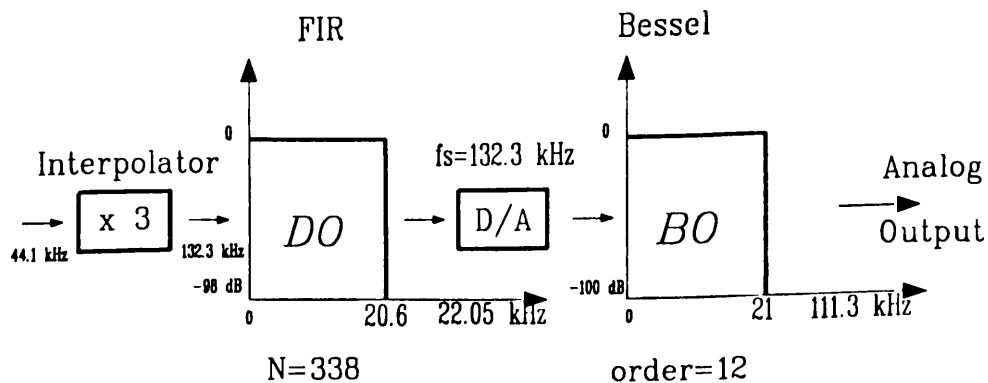
where  $\hat{H}(e^{j\omega})$  is a real-valued function, and  $\beta$  and  $\sigma$  are both constants. In [4] it is proved that the only solutions for these constants are  $\sigma = (N - 1)/2$ ,  $\beta = 0$  (corresponding to a symmetrical impulse response), and  $\beta = \pi/2$  (corresponding to an antisymmetrical im-



(a)



(b)



(c)

Fig. 2. Digital audio equalizer system. (a) Input stage. (b) Equalizer stage. (c) Output stage.

pulse response).

Since we are only interested in the symmetrical case, Eq. (6) can be rewritten as

$$H(e^{j\omega}) = \hat{H}(e^{j\omega}) e^{-j\sigma\omega} \tag{7}$$

In this equation the term  $\sigma$  is the group delay [defined in Eq. (1)], and it has been noticed that it is a constant. Thus FIR filters can be designed with constant group delay (that is, phase linear).

Using trigonometric identities, it can be shown that  $H(e^{j\omega})$  can be expressed as a linear combination of weighted cosines, or

$$\hat{H}(e^{j\omega}) = \begin{cases} \sum_{n=0}^{(N-1)/2} a(n) \cos(\omega n), & N \text{ odd} \\ \sum_{n=1}^{N/2} b(n) \cos[\omega(n - 1/2)], & N \text{ even} \end{cases} \tag{8}$$

where

$$\begin{aligned} a(0) &= h(M) \\ a(n) &= 2h(M - n), \quad n = 1, 2, \dots, M \\ b(n) &= 2h(\hat{M} - n), \quad n = 1, 2, \dots, \hat{M} \end{aligned}$$

and

$$M = \frac{N - 1}{2}, \quad \hat{M} = \frac{N}{2}$$

Consequently, since the linear-phase term in Eq. (7) is a constant and has no effect on the magnitude response of the FIR filter, we only need to consider the appropriate form of Eq. (8) in order to approximate a desired frequency response.

The design of an FIR filter can be achieved by finding its impulse response coefficients or  $N$  samples of its frequency response. The implementation of FIR filters,

however, usually requires a very large number of coefficients, which in turn demands large computation times that may not be supported by currently available hardware.

## 2 FILTER REQUIREMENTS

An important criterion in the design of high-fidelity digital audio is to create a system capable of handling all signal source characteristics, even those that may be highly improbable. The system must accommodate changes in sound characteristics due to sound effects (for example, the new variety of digital sounds reproduced in the recording of motion pictures) or synthesized sounds that can exceed the limits of human hearing. This suggests that the dynamic range available with digital techniques may very well exceed 100 dB. Therefore, the ideal high-fidelity digital audio filter must have the flattest passband response (to at least  $\pm 0.1$  dB) in order to avoid waveform degradation, as well as attenuate all signals beyond the Nyquist frequency by about 100 dB (the available dynamic range with 16-bit digitization) to avoid aliasing effects, and must be phase linear to preserve audio fidelity. Fig. 4 shows the desired specifications for a prototype low-pass filter. In the design of FIR filters we are concerned with the following parameters: filter length  $N$ , stopband cutoff frequency  $F_s$ , passband cutoff frequency  $F_p$ , passband ripple  $\delta_1$ , and stopband attenuation  $\delta_2$ .

## 3 FIR FILTER DESIGN

The design of an FIR filter can be accomplished through methods such as frequency sampling or windowing; however, the flexibility offered by such techniques is very limited. The difficulty found in the design of FIR filters with stringent requirements for passband ripple and stopband attenuation lies not only in the fact that we must maintain control over the parameters in-

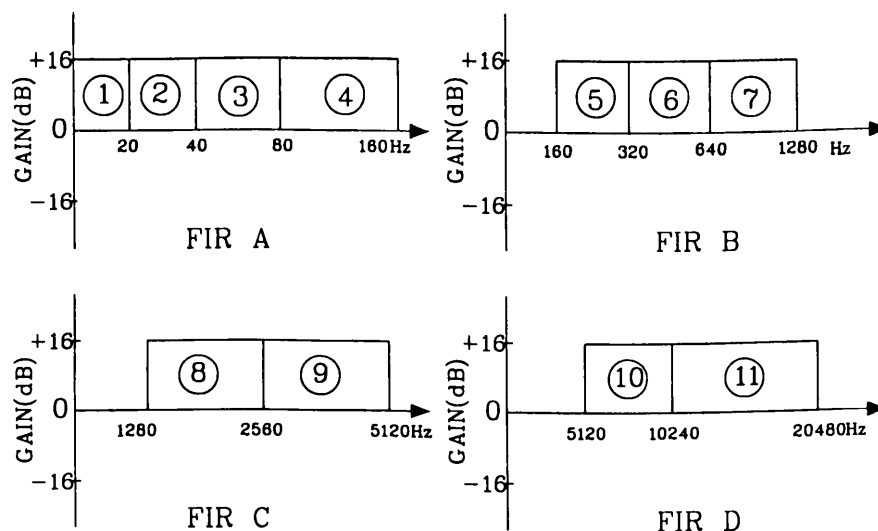


Fig. 3. Digital equalizer structure. Audio spectrum is separated into four bands and each band can be adjusted for a  $\pm 16$ -dB gain.

involved such as the cutoff passband and stopband frequencies, but most importantly, in the knowledge that we must keep the coefficients down to a reasonable number for purposes of hardware implementation.

In order to have control over the parameters involved, a powerful and sophisticated method of design is found in a numerical approximation technique known as the Remez exchange method. This technique is the basis of a program developed by McClellan, Parks, and Rabiner [5] for the design of FIR filters with linear phase. All digital filters in our study are optimally designed using the Remez exchange method as implemented in this program. This technique is not only capable of designing any optimal filter (where "optimal" refers to the approximation with the least maximum error, also called the Chebyshev norm), but it also allows the designer control over parameters  $N$ ,  $F_s$ , and  $F_p$  by allowing the error deviations ( $\delta_1$  and  $\delta_2$ ) to vary about some desired value of gain. The freedom to choose the exact location of the cutoff frequencies as well as the desired number of coefficients is what makes this method very powerful and more efficient over other methods of design.

### 3.1 Formulation of Optimization Problem

The design of FIR filters with linear phase can be stated as a Chebyshev approximation problem by first defining the following functions:

- $H_d(e^{j\omega}) \triangleq$  desired frequency response of filter
- $H(e^{j\omega}) \triangleq$  best frequency response approximation
- $W(e^{j\omega}) \triangleq$  positive weighting function, which determines penalty on error
- $E(e^{j\omega}) \triangleq$  weighted error function.

These functions are continuous on a closed subset of  $[0, \frac{1}{2}]$  (where the sampling frequency  $f_s$  has been normalized to 1).

The expression for the weighted error function can be written as [5]

$$E(e^{j\omega}) = W(e^{j\omega}) [H_d(e^{j\omega}) - H(e^{j\omega})] . \quad (9)$$

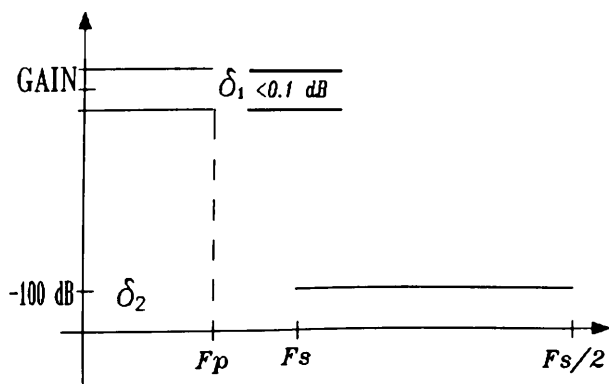


Fig. 4. Specifications of prototype low-pass filter showing requirements for passband and stopband attenuation.

The design problem consists of finding the set of impulse response coefficients  $\{a(n), b(n)\}$  in Eq. (8) which minimize the objective function:

$$\|E(e^{j\omega})\| = [\max_{\omega \in \mathcal{W}} |E(e^{j\omega})|] \quad (10)$$

where  $\mathcal{W}$  is a closed subset of  $[0, \frac{1}{2}]$ , and  $\|E(e^{j\omega})\|$  denotes the  $L_\infty$  norm of  $E(e^{j\omega})$ .

Since the problem is to minimize the maximum absolute value of  $E(e^{j\omega})$  over the frequency bands of interest (namely,  $0-F_p$  and  $F_s-f_s/2$  for the low-pass case), and since this maximum is  $\delta$ , then Eq. (9) can be written as

$$W(e^{j\omega_i}) [H_d(e^{j\omega_i}) - H(e^{j\omega_i})] = (-1)^i \delta , \quad (11)$$

$$i = 0, 1, 2, \dots, N .$$

If we can find the points along the frequency grid which satisfy this equation, we can then reconstruct the frequency response from Eq. (8), perform an inverse discrete Fourier transform (DFT), and obtain the coefficients corresponding to the optimal approximation. The Remez exchange algorithm is a fast and efficient numerical method for the location of these frequency points.

The necessary and sufficient conditions for the solution of Eq. (11) are given by the so-called alternation theorem [6]. This theorem restricts the number of frequency points along which the error oscillates, thus facilitating the location of extrema. The theorem applies to expressions such as Eq. (8), in which the polynomial  $H(e^{j\omega})$  is expressed as a linear combination of  $N$  cosine basis functions. The optimal solution is then found by applying the Remez exchange algorithm in order to find the Chebyshev (or minimax) approximation to the desired function  $H_d(e^{j\omega})$ . The method iteratively searches for the location of extrema (note that the alternation theorem restricts this number of extrema) until Eq. (11) is satisfied and the desired error deviation is achieved.

In [5] this method is implemented in a program in which the filter size, the cutoff frequencies, the desired frequency response in each band, and the corresponding penalty function are input. In turn, the output consists of the impulse response coefficients of the best approximation, the optimal error ( $\min \|E(e^{j\omega})\|$ ), and the extremal frequencies where  $E(e^{j\omega}) = \pm \|E(e^{j\omega})\|$ . In this way individual low-pass or multiband FIR filters can be designed.

Using this method, each of the FIR filters needed in the implementation of the 11-band audio equalizer can be designed to satisfy the requirements for  $\delta_1$ ,  $\delta_2$ , and cutoff frequencies, given a number of coefficients  $N$ . However, some problems still remain:

1) There is a large deviation from flat response at the band crossing (or composite) region when two or more bands are set to the same gain (see Fig. 1).

2) The anti-aliasing and anti-imaging filters needed to support the equalizer stage of the system must also meet strict requirements for passband ripple and stop-



band attenuation. Consider, for example, that if the audio signal is sampled at 44.1 kHz, with  $\delta_1 = \pm 0.1$  dB and  $\delta_2 \geq 100$  dB beyond the Nyquist frequency, the analog anti-aliasing filter needed would require a rolloff rate of more than 700 dB per octave, or more than 116 poles, for its realization. Not only is such a filter difficult to implement, but the steep rolloff rate will introduce phase nonlinearities.

3) The number of coefficients  $N$  required for the implementation of each FIR filter remains prohibitively large. For instance, if the sampling frequency is 44.1 kHz, the number of coefficients required to implement a low-pass filter in the equalizer stage (0–20 Hz, 25–22 050 Hz) will range from 29 859 (for  $\delta_1 = \pm 0.1$  dB and  $\delta_2 = -90$  dB) to 32 478 (for  $\delta_1 = \pm 0.1$  dB and  $\delta_2 = -100$  dB). See Appendix.

Nevertheless, in order to resolve these problems we implement the filter structure initially proposed in [7], combined with the use of decimating and interpolating techniques, and the modification of the McClellan, Parks, and Rabiner program as explained in the following section.

### 3.1.1 Parallel Filter Structure

In this design, the audio spectrum is divided into four separate bands, dc–160 Hz, 160–1280 Hz, 1280–5120 Hz, and 5120–20 480 Hz, consisting of 11 filters which allow individual control over each of the 11 octaves covering the full range of left and right channels (0–20 480 Hz). Each of the four bands is designed by a set of FIR filters having an adjustable bandpass gain of  $\pm 16$  dB, and each filter uses samples which are taken at an integer multiple of 44.1 kHz (see Fig. 3).

The parallel structure allows the overall filter characteristics to be changed on line by modifying the coefficients of one bandpass filter. Each filter is implemented by convolving its coefficients with data points, thus allowing the addition of the coefficients from each band. For example, Fig. 5 represents the addition of two parallel filters with impulse responses  $h_1(k)$  and  $h_2(k)$ . If  $x(k)$  is the input signal, the output is then given by

$$y(k) = \sum_{r=1}^N h_1(r)x(k-r) + \sum_{r=1}^N h_2(r)x(k-r) \quad (12)$$

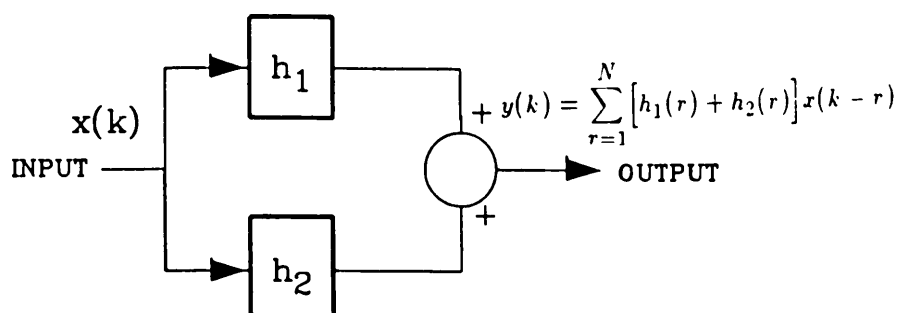


Fig. 5. Addition of two parallel filters. Addition of two or more symmetrical impulse responses preserves phase linearity.

This equation can be written as

$$y(k) = \sum_{r=1}^N [h_1(r) + h_2(r)]x(k-r) \quad (13)$$

Each digital filter in this system is designed as symmetric FIR, and therefore each has linear phase. The addition of two or more symmetric impulse responses results in a symmetric impulse response also [see Eq. (13)]. Therefore the parallel filter structure preserves phase linearity.

The structure just described relaxes the constraint incurred in the design by the number of coefficients and makes possible the realization of sharp, selective FIR digital filters that can be implemented with commercially available hardware. Experimental results show that using this technique, all filters in the equalizer stage can be designed with  $N = 356$  while keeping  $\delta_1 \leq 0.1$  dB and  $\delta_2 \leq -95$  dB.

### 3.1.2 Decimation and Interpolation

The digital equalizer system constitutes a multirate digital filter bank, which means that throughout the system the sampling rate does not remain constant. This process allows the use of low-order analog filters in order to eliminate the images produced by the sampling process of the A/D and D/A converters.

In the stage following A/D conversion, the sampling rate is reduced in order to match the required frequency corresponding to each parallel filter path (refer to Figs. 2 and 5). In the stage preceding D/A conversion, the sampling rate is increased in order to match the required sampling rate. The reduction in sampling rate is achieved by the process of decimation (undersampling), while the increase is achieved by interpolation (oversampling).

Decimation/interpolation systems consist of digital filters in which the input and output rates are different. For example, for a  $D$ -fold decimation (reducing the sampling frequency from  $f_s$  to  $f_s/D$ ), a decimator system takes in a sequence  $x(n)$  and produces a compressed (in time) sequence  $y(n) = x(Dn)$  by retaining only those input samples which are integer multiples of the decimator factor  $D$ . Similarly, for an  $I$ -fold interpolation (increasing the sampling frequency from  $f_s$  to  $I f_s$ ), an interpolator system takes in a sequence  $x(n)$  and produces a stretched (in time) sequence  $y(n) = x(n/I)$  by

inserting  $I - 1$  zero-valued samples for each pair of input samples.

### 3.1.3 Technique for Obtaining All Filters

We recall from Sec. 2 that the parameters involved in the design of optimal FIR filters are impulse response duration in number of samples  $N$ , stopband cutoff frequency  $F_s$ , passband cutoff frequency  $F_p$ , passband deviation  $\delta_1$ , and stopband deviation  $\delta_2$ . Several important methods have been developed which extend the design capabilities of the McClellan, Parks, and Rabiner computer program for the design of optimal FIR filters. In [6] an estimated value for  $N$  (see Appendix) is calculated in order to meet given values of  $F_s$ ,  $F_p$ ,  $\delta_1$ , and  $\delta_2$  for FIR low-pass filter design. In [8] this method is extended to the multiband filter design case, and in [9] an optimal FIR low-pass filter can be designed where any four of the five filter parameters are specified, and the remaining one can be chosen to meet a desired specification.

All these methods introduce a set of simple formulas that can be used to vary an unspecified parameter from its initial estimate in order to meet required filter specifications within a given tolerance. In our study, similar techniques have been adopted to accommodate the required specifications of filter size of 356 coefficients, stopband attenuation of  $-98$  dB, and passband ripple of about  $0.08$  dB for each FIR filter in the equalizer stage. (The input/output filters have been designed with the same restrictions, except that the number of coefficients is less than 356, as explained later.) The method is extended, however, in order to consider the composite response constraint which restricts the error deviation within this region to  $\pm 0.2$  dB (see Fig. 6).

Unfortunately all these specifications cannot be met at the same time. When the individual filters for the equalizer stage are designed, it is found that each filter can be designed to satisfy the given requirements. However, when coefficients of adjacent bands are added together, the composite frequency response shows unacceptable error deviations. Therefore a compromise has to be made allowing the values of  $N$ ,  $\delta_1$ , and  $\delta_2$  to

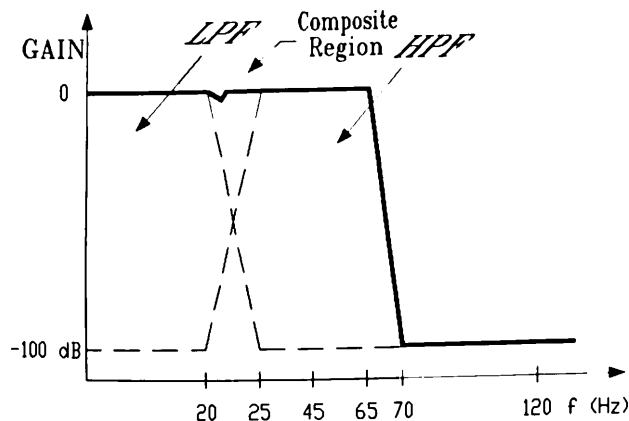


Fig. 6. Example showing overall response of adjacent filters and requirements for amplitude deviation at band crossings.

remain as specified, but allowing the stopband frequencies to change slightly in order to accommodate the composite response constraint.

The justification for this technique can be explained by first considering two additional useful filter parameters, the transition width  $\Delta F = F_s - F_p$  and the deviation ratio  $K = \delta_1/\delta_2$ . This last quantity allows us to choose the weight function in Eq. (11) as follows [3]:

$$W(e^{j\omega}) = \begin{cases} 1/K, & \text{passband} \\ 1, & \text{stopband} \end{cases} \quad (14)$$

forcing  $H(e^{j\omega})$  to interpolate to

$$H(e^{j\omega}) = \begin{cases} 1 \pm K\delta, & \text{passband} \\ \pm \delta, & \text{stopband} \end{cases} \quad (15)$$

where  $\delta$  is the desired stopband attenuation.

Experiments show [5] that a small variation of one of the parameters  $\Delta F$  or  $K$  can result in a significant reduction of the error while keeping  $N$  constant. Since we have agreed to keep  $\delta_1$  and  $\delta_2$  unchanged, and we have consequently decided on a value for  $K$ , we then opt for the possibility of varying  $\Delta F$  (or  $F_s$ ) until a satisfactory error deviation is attained. The algorithm developed calculates the coefficients needed for the design of two adjacent bands. These coefficients are calculated for each filter based on the required parameters. When the stopband frequencies  $F_s$  of the bands are changed from an initial estimate, a point is reached where the deviation in the composite region attains  $\pm 0.2$  dB while the rest of the parameters remain virtually unchanged.

The algorithm first calculates the initial  $F_s$  estimate [see Appendix, Eq. (21)] for each filter of the equalizer stage. All filter parameters are input into the program and the impulse response coefficients corresponding to each filter are estimated by the Remez exchange method. Next the coefficients are added together and their frequency response computed. The program then checks the deviation in the composite region. If this deviation is not within  $\pm 0.2$  dB, then  $F_s$  is changed from its initial estimate and the Remez algorithm is recalled in order to calculate the coefficients of the best response. The algorithm iteratively calculates the deviation within the composite region, varying  $F_s$  until the desired deviation is found.

The result of applying these ideas to the filters shown in Fig. 7(a), where the deviation in the composite region reaches  $-8$  dB, can be seen in Fig. 7(b) and (c). In this case the deviation is reduced to an average  $\pm 0.1$  dB, reaching a maximum of  $\pm 0.2$  dB as desired.

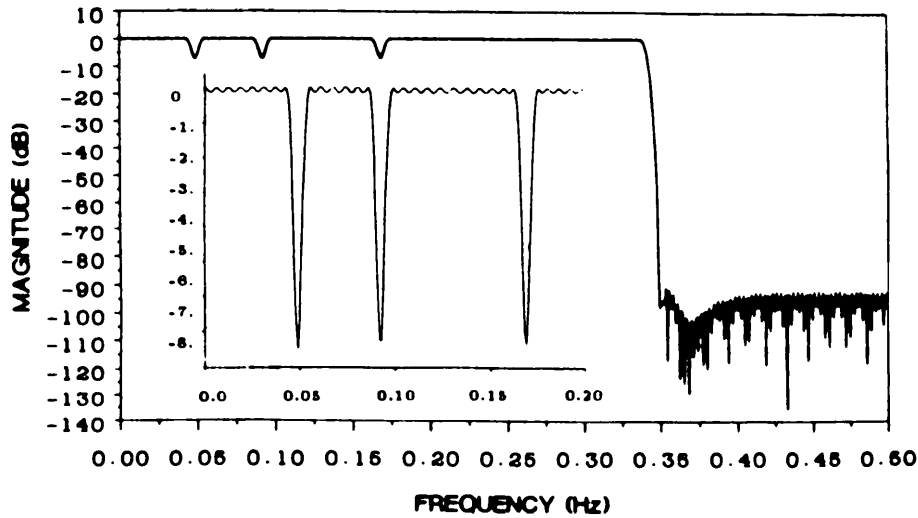
## 4 PRESENTATION OF RESULTS

We have seen that the design obstacles encountered in the development of the equalizer system can be resolved by the methods discussed. We now discuss a technique to select the final filter parameters that will

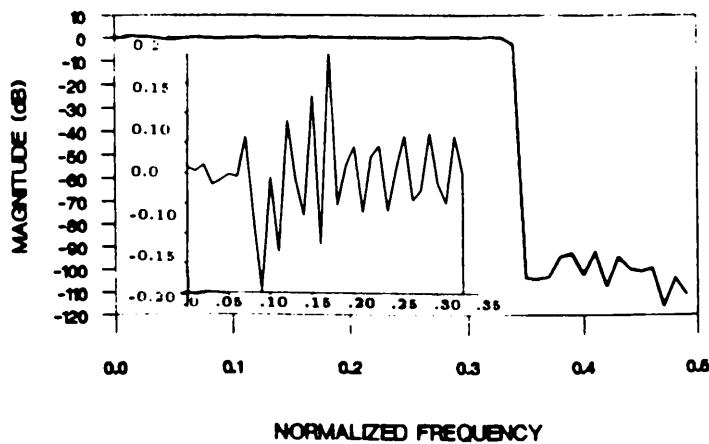
result in the best overall design, namely, cutoff frequencies for anti-aliasing filters, system sampling frequencies, and so on.

The audio equalizer constitutes a system in which all the elements of the signal path are synchronized in order to produce the best overall design. In that respect, the particular sampling frequency for each of the four

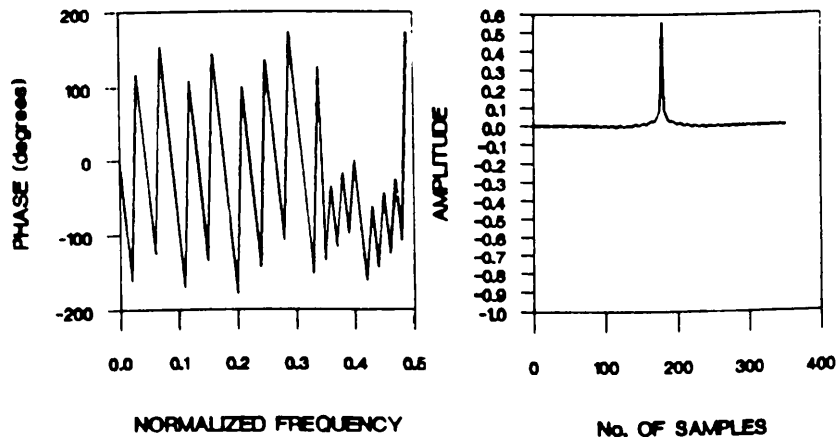
parallel paths has to be chosen taking into consideration every frequency band along the particular path. We should recall that the use of oversampling allows us to move the stopband cutoff point down in frequency so that a low-order anti-aliasing filter can be used. Such a filter must be phase linear and suited to the required characteristics for passband and stopband frequencies.



(a)



(b)



(c)

Fig. 7. (a) Composite frequency response of four adjacent filters without modification of stopband frequencies. Deviation from flat response is near 8 dB. (b) Same composite response after modification of stopband frequencies by method explained in Sec. 3.13. Deviation is now less than 0.2 dB. (c) Symmetry of impulse response and phase linearity are preserved.

It is also recalled that all sampling frequencies are integer fractions of 44.1 kHz.

To apply these ideas to our design, consider path 1 as shown in Fig. 2. First, in order to obtain a low-order analog anti-aliasing filter, we settle for a sampling frequency of 5512.5 Hz (or an oversampling factor of 12 with respect to the equalizer sampling frequency for this path). The sampling frequency just chosen results in the best compromise between the rolloff of Bessel filter A (and thus the number of poles), and the number of coefficients needed to generate FIR-DA (this latter filter is needed prior to undersampling).

Now, by choosing the stopband frequency for Bessel filter A at 2756.25 Hz, the cutoff passband frequency at 180 Hz (to ensure that the passband region will cover the entire spectrum for this path), and a stopband attenuation of about 100 dB, the required rolloff rate is approximated by the following expression:

$$\text{stopband attenuation (in dB)} \frac{\log 2}{\log [(f_s - F_s)/F_p]} \quad (16)$$

where  $f_s$  represents the sampling frequency and the rolloff rate is given in decibels per octave.

If we use all the parameters just determined and apply the preceding expression, we then obtain a rolloff of  $\sim 25.40$  dB per octave for Bessel filter A, which in turn requires a five-pole filter for its realization (recall that each pole provides a rolloff of 6 dB per octave approximately). For a more accurate result, however, the number of poles needed for each Bessel-Thomson filter is also corroborated experimentally. These numbers are also shown in Fig. 2.

Now since we must also decimate by a factor of 12, the requirements of anti-aliasing filter FIR-DA must be such that the stopband cutoff frequency is equal either to  $f_s/2D$  (where  $D$  is the decimation factor) or to  $f_s/2$ , whichever is less. Therefore, for  $D = 12$  and  $f_s = 5512.5$  Hz the required stopband frequency must be at  $\sim 229.68$  Hz. This finding, together with the other parameter information such as stopband attenuation, passband deviation, and cutoff frequency, can be combined in order to obtain an approximation for the required FIR filter length that will result in the desired frequency response. This information is then used in Eq. (21) (see Appendix) in order to obtain  $N = 342$ . Lastly, a decimation factor of 12 results in a sampling frequency of 459.375 Hz for path 1 of the equalizer stage. Again, this decimation factor results in the best compromise between the sampling frequency and the required filter characteristics so that the filter length is kept to a minimum.

At this point we have reached a compromise among all the filter parameters along path 1, and we have determined all the required characteristics needed to design such filters. A similar approach can be applied to the remaining equalizer paths in order to develop the entire system. For simplification in the analysis,

all filter specifications are included in Fig. 2.

By implementing the algorithm presented in the previous section and with all the system parameters established, we are able to design all filters with the required characteristics. Fig. 8 shows the responses (magnitude, phase, and impulse) corresponding to some of the bands of the equalizer and input stages. Several examples showing the effects of positioning the equalizer bands at different settings of gain are also included in Fig. 9. The results presented here show that the system is capable of maintaining the required characteristics for phase, passband, and stopband attenuation well within the limits previously established in this study.

## 5 HARDWARE IMPLEMENTATION

The block diagram corresponding to the equalizer system is shown in Fig. 10. This figure also shows all the sampling frequencies used in the design. The hardware implementation for changing the coefficients is suggested in Fig. 11. In this configuration, the individual filter coefficients (as obtained from the method described in Sec. 4) are stored in EPROM, while RAM is used to store the audio samples. The microprocessor ( $\mu P$ ) is continuously scanning the position of the potentiometer settings. Whenever a gain position is changed, the  $\mu P$  uses the new setting to look up the new coefficients in a table in the EPROM. From the A/D converter, the data samples are stored in RAM. The control logic circuit communicates with the  $\mu P$  so that new coefficients (depending on the gain) are written into a coefficient buffer, and input samples into a sample buffer. The filter coefficients and data samples are then passed to a multiplier accumulator (MAC) for the purpose of increasing the speed of the process.

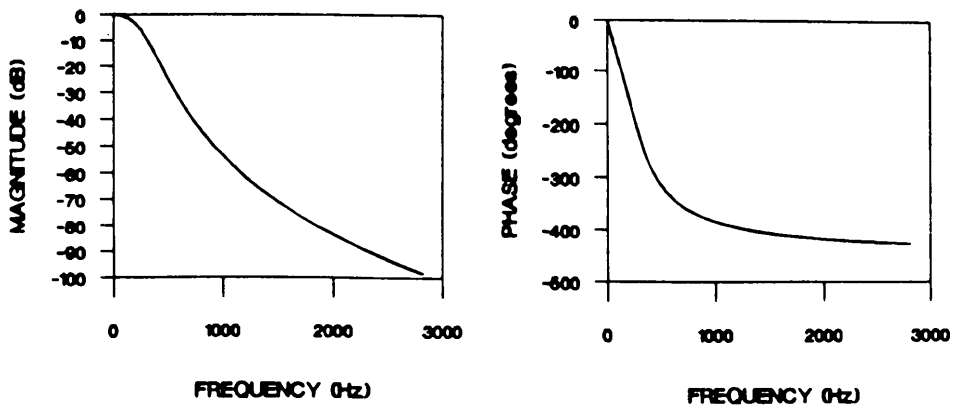
We must still consider the speed requirements needed for the MAC in order to support the established sampling rates. To make this decision, we first calculate the multiplication rate required for each of the four paths considered in our design. The number of multiplications per second equals the sampling rate times the number of coefficients. Consider, for example, FIR A in Fig. 2. The sampling frequency is 459.375 Hz, and the number of multiply/accumulates is thus  $459.375 \times 356 = 163\,537.5$ . The processing time per multiply/accumulate is therefore  $1/(163\,537.5) = 6.11 \mu s$ . In the same manner, we determine a multiply/accumulate time of 765 ns for FIR B, 127 ns for FIR C, and 64 ns for FIR D. The operation time required for FIR D can be accommodated by the use of Analog Device's ADSP-1010B MAC. This device is a high-speed CMOS MAC with a multiply/accumulate time of 45 ns and a power dissipation rate of 170 mW.

## 6 CONCLUSIONS

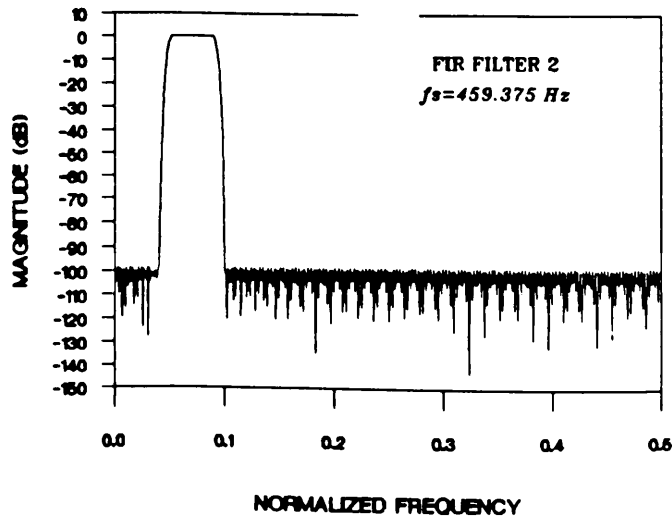
An 11-band digital audio equalizer has been designed which exhibits both phase linearity and interband gain independence. The design approach in this study con-

sists of using the Remez exchange algorithm iteratively and in varying the transition width of each FIR filter of the equalizer in order to meet established requirements for error tolerance in the passband, stopband, and composite regions. Several examples show that the system maintains the phase requirements of  $\delta_1 =$

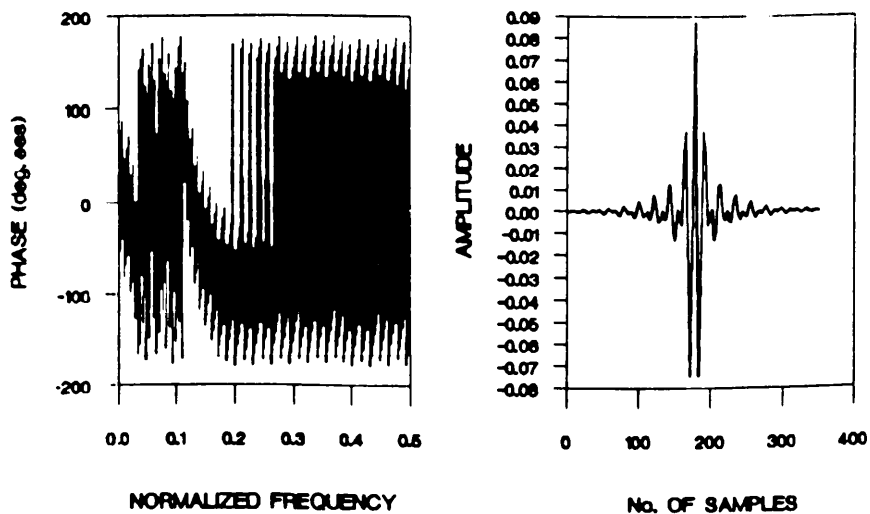
$\pm 0.1$  dB for individual filters, and  $\pm 0.2$  dB in composite regions, and also of  $\delta_2 \sim -100.00$  dB. These results are even more impressive when compared to analog equalizer designs. The techniques described in this paper reduce the filter size considerably, thus allowing the use of currently available hardware for im-



(a)



(b)



(c)

Fig. 8. Typical behavior obtained from design of analog and digital filters. (a) Frequency response for anti-aliasing Bessel filter A. (b) Frequency response corresponding to FIR band 2 of equalizer. (c) Linearity of phase and symmetry of impulse response expected.

plementation. It is the hope of the authors that the methods applied to the solution of the problems encountered in the design of this system can be implemented and improved upon in the development of similar digital audio systems.

## 7 REFERENCES

- [1] D. Preis and P. J. Bloom, "Perception of Phase Distortion in Anti-Alias Filters," *J. Audio Eng. Soc.*, vol. 32, pp. 842–848 (1984 Nov.).
- [2] J. Meyer, "Time Correlation of Anti-Aliasing Filters Used in Digital Audio Systems," *J. Audio Eng. Soc. (Engineering Reports)*, vol. 32, pp. 132–137 (1984 Mar.).
- [3] A. V. Oppenheim and R. W. Schaffer, *Digital Signal Processing* (Prentice-Hall, Englewood Cliffs, NJ, 1985), chap. 5.
- [4] J. McClellan and T. W. Parks, "A Unified Approach to the Design of Optimum FIR Linear-Phase Digital Filters," *IEEE Trans. Circuit Theory*, vol. CT-20, pp. 697–701 (1973 Nov.).
- [5] J. H. McClellan, T. W. Parks, and L. R. Rabiner, "A Computer Program for Designing Optimum FIR Linear-Phase Digital Filters," *IEEE Trans. Audio Electroacoust.*, vol. AU-21, pp. 506–526 (1973 Dec.).
- [6] T. W. Parks and J. H. McClellan, "Chebyshev Approximation for Nonrecursive Digital Filters with Linear Phase," *IEEE Trans. Circuit Theory*, vol. CT-19, pp. 189–194 (1972 Mar.).
- [7] T. E. Riemer, R. E. Trahan, and B. G. Ragan, "Design of a Phase-Linear Digital Audio Equalizer," presented at the 74th Convention of the Audio Engineering Society, *J. Audio Eng. Soc. (Abstracts)*, vol. 31, p. 970 (1983 Dec.), preprint 2039.
- [8] L. Rabiner, J. Kaiser, and R. Schaffer, "Some Considerations in the Design of Multiband Finite-Impulse-Response Digital Filters," *IEEE Trans. Acoust., Speech, Signal Process.*, vol. ASSP-22, pp. 462–472 (1974 Dec.).
- [9] L. R. Rabiner, "Approximate Design-Relations for Low-Pass FIR Digital Filters," *IEEE Trans. Audio Electroacoust.*, vol. AU-21, pp. 456–460 (1973 Oct.).

## APPENDIX FILTER-LENGTH PREDICTION FORMULA FOR FIR FILTER DESIGN

A very accurate formula for approximating the number of coefficients  $N$  required in the design of low-pass FIR filters is due to Herrmann et al. (see [6]). This

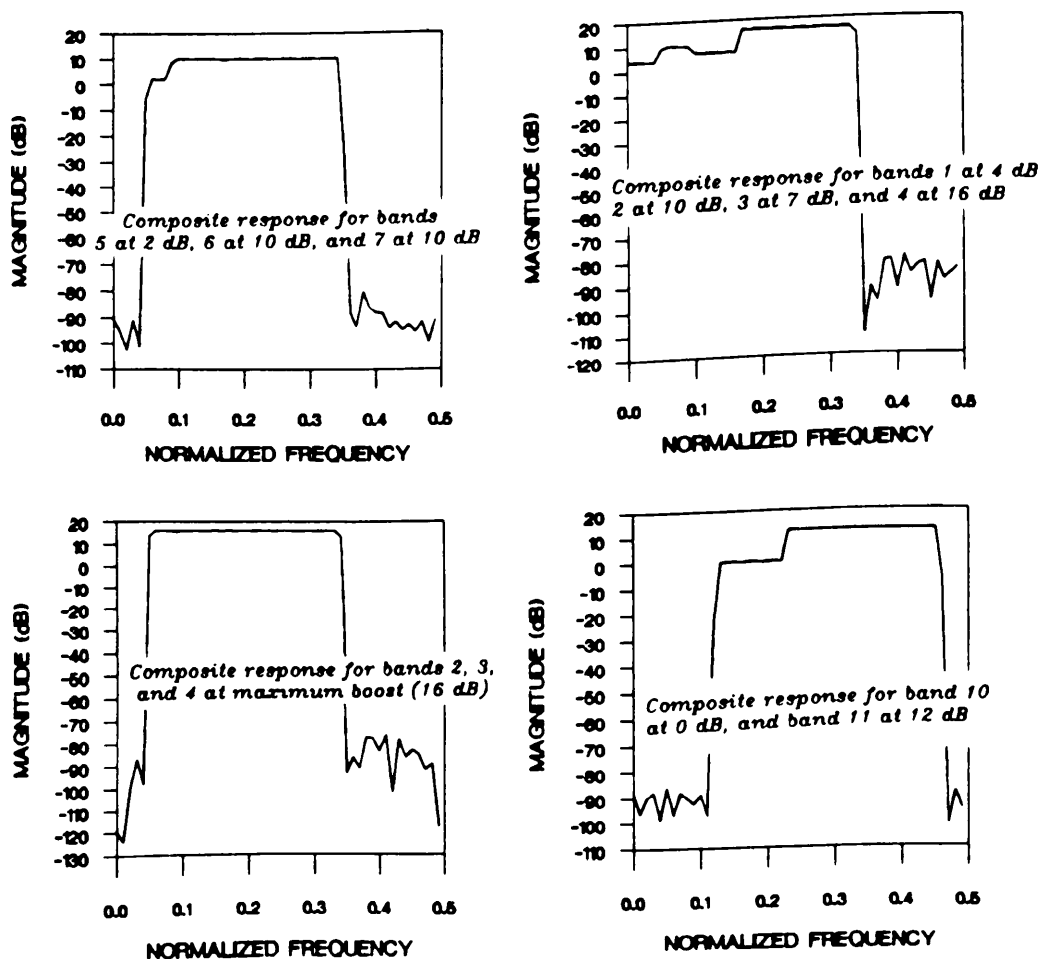


Fig. 9. Behavior of digital audio equalizer at different gain settings. System maintains required characteristics for phase, passband, and stopband attenuation.

formula sets a relation between all five parameters needed for the filter approximation and can be stated by first defining the following constants:

$$\begin{aligned} A_1 &= 5.309^{E-03} & A_2 &= 7.114^{E-02} \\ A_3 &= -4.761^{E-01} & A_4 &= -2.66^{E-03} \\ A_5 &= -5.941^{E-01} & A_6 &= -4.278^{E-01} \\ B_1 &= 11.012 & B_2 &= 0.51244 \end{aligned} \quad (17)$$

All these constants were determined empirically by applying a minimum mean-square error fitting procedure. Also letting

$$\begin{aligned} \text{DEVI}_1 &\triangleq \log_{10} \delta_1 \\ \text{DEVI}_2 &\triangleq \log_{10} \delta_2 \end{aligned} \quad (18)$$

where  $\delta_1$  is the desired passband deviation and  $\delta_2$  is

the desired stopband deviation. Now let

$$\begin{aligned} \phi &\triangleq [A_1(\text{DEVI}_1)^2 + A_2(\text{DEVI}_1) + A_3] \text{DEVI}_2 \\ &+ [A_4(\text{DEVI}_1)^2 + A_5(\text{DEVI}_1) + A_6] \end{aligned} \quad (19)$$

and

$$\chi \triangleq B_1 + B_2(\text{DEVI}_1 - \text{DEVI}_2) \quad (20)$$

Using these expressions the formula approximating the optimal filter length is then given by

$$N = \frac{\phi - \chi \Delta F^2}{\Delta F} + 1 \quad (21)$$

where  $\Delta F = F_s - F_p$  is the transition width.

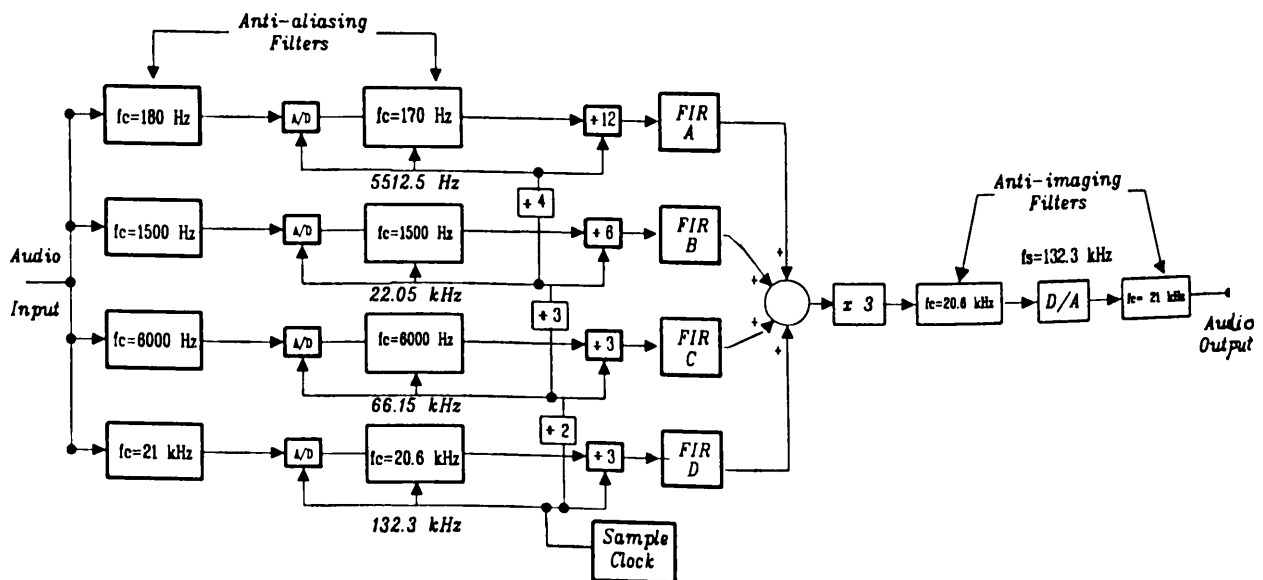


Fig. 10. Block diagram of phase-linear digital audio equalizer.

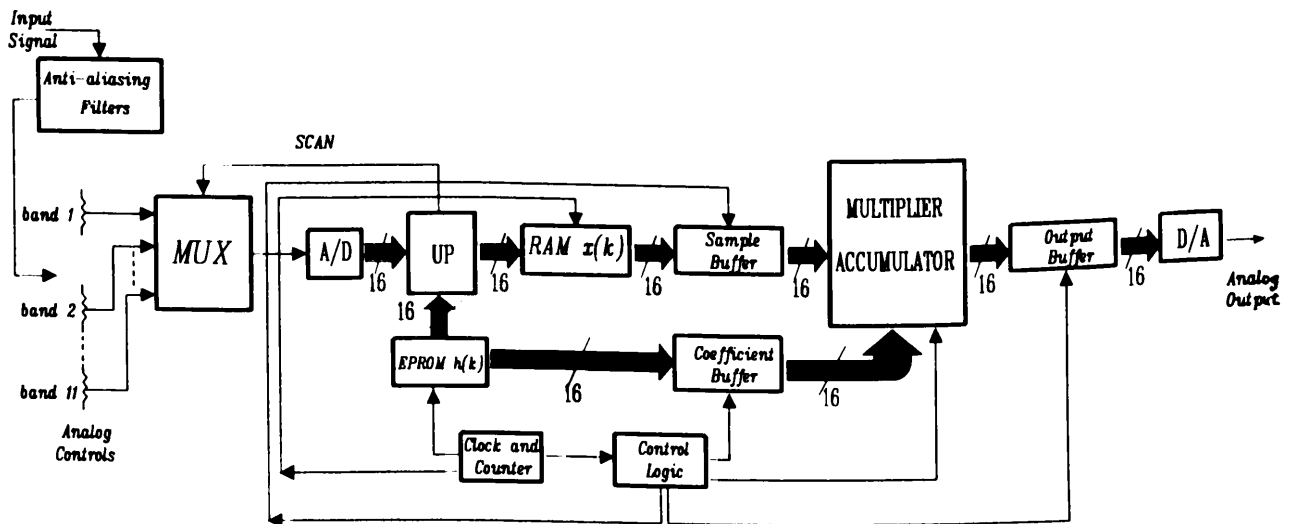


Fig. 11. Hardware implementation of phase-linear digital audio equalizer.

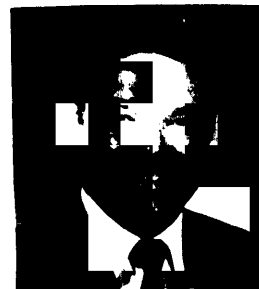
## THE AUTHORS



J. A. Henriquez



T. E. Riemer



R. E. Trahan, Jr.

Juan A. Henriquez was born in San Salvador, El Salvador, on May 27, 1960. He holds a B.S. degree in electrical engineering and an M.S. degree in engineering, both from the University of New Orleans, New Orleans, Louisiana, where he works as a part-time instructor in the Department of Electrical Engineering. His research interests include digital signal processing, audio, and control systems.

He is a member of the AES, IEEE, and an associate member of the ASA.

Terry E. Riemer received B.S.E.E. and M.S.E.E. degrees from Tulane University, New Orleans, Louisiana, and a Ph.D. in electrical engineering from Purdue University, LaFayette, Indiana. From 1970 to 1974 he was a graduate researcher at the Laboratory for Application of Remote Sensing (LARS), Purdue University, and an instructor in electrical engineering at Purdue University. From 1974 to 1975 he was employed at the Bellaire Research Laboratory of Texaco, Inc., Houston, Texas, where he was involved in the development of seismic data processing algorithms based upon signal and image processing techniques. In 1975 he joined the faculty of the University of New Orleans where he is currently associate professor of electrical

engineering.

Dr. Riemer's teaching and research interests are in the areas of audio electronics, communications, and the application of signal and image processing techniques to biomedicine, geophysics, speech, and audio.

Russell E. Trahan, Jr. was born in New Orleans, Louisiana on January 30, 1949. He obtained the B.S. and M.S. degrees in engineering from the University of New Orleans in 1970 and 1973 respectively. He then obtained a Ph.D. in electrical engineering from the University of California at Berkeley in 1977. He has been on the faculty at the University of New Orleans since 1977 where he holds the rank of professor of electrical engineering. During the summers of 1986, 1987, 1988, and 1989 he was awarded a Navy/ASEE Summer Faculty Fellow position at the Naval Ocean Research and Development Activity (NORDA) at Stennis Space Center, Mississippi. He has continued as a consultant to the Advanced Technology Branch of NORDA since 1987. His research interests include optimization, controls, and signal processing.

He is a member of IEEE (currently chairman of the New Orleans section), ASEE, ISA, Eta Kappa Nu, Phi Kappa Phi, and Omicron Delta Kappa.